

Flood and earthquake disturbance of ^{210}Pb geochronology (Lake Anterne, NW Alps)

F. Arnaud,^{1,3*} V. Lignier,^{2,3} M. Revel,^{2,4} M. Desmet,^{2,3} C. Beck,^{2,3} M. Pourchet,⁵ F. Charlet,^{1†} A. Trentesaux¹ and N. Tribouvillard¹

¹*Bilan et Processus en Domaine Sédimentaire UMR CNRS, Université de Lille 1, F-59655 Villeneuve d'Ascq Cedex,* ²*Laboratoire de Géodynamique des Chaînes Alpines, UMR CNRS 5025,* ³*Université de Savoie, F-73376 Le Bourget du Lac Cedex,* ⁴*OSUG, Université J. Fourier, F-38400 Saint Martin d'Hères Cedex,* ⁵*Laboratoire de Glaciologie et Géophysique de l'Environnement, UMR CNRS 5511, F-38402 Saint Martin d'Hères Cedex, France*

ABSTRACT

Dating recent lake sediment records yielding disturbed ^{210}Pb profiles has been a problem of wide interest in palaeoclimatic and palaeoseismic studies over the last few centuries. When applied to an alpine lake sedimentary record, a high-resolution sedimentological study reveals that the ^{210}Pb profile is disturbed by the occurrence of single-event deposits triggered by two different mechanisms: flood events deposits and gravity reworking. Removing disturbed layers from the ^{210}Pb profile yields a logarithmic depth–activity relationship. Using a simple ^{210}Pb decay model (CFCS) provides an assessment of mean

accumulation rate of 'continuous sedimentation', as opposed to 'event-linked sedimentation'. The correlation of the thickest four gravity-reworked deposits with historically known earthquakes permits both validation and refinement of the age–depth relationship. This refinement highlights variations in accumulation rate consistent with post-Little Ice Age climatic variations.

Terra Nova, 14, 225–232, 2002

Introduction

Recent investigations concerning past climate variability (Von Grafenstein *et al.*, 1996; Chapron *et al.* 2002) and/or seismic activity (Doig, 1990; Chapron *et al.*, 1999) over the last millennia have pointed out the importance of lacustrine sediment records for providing proxy time-series with annual to decadal resolution over a millennial timescale, allowing an accurate chronology to be established (Smith, 2001). Classically, on millennial timescales, sedimentation rate is extrapolated from the last century average rate inferred from ^{210}Pb chronology.

Since the first application of ^{210}Pb radiochronology to lake sediments (Krishnaswamy *et al.*, 1971), it has become an indispensable tool for dating recent sediments (Noller, 2000). Three ^{210}Pb dating models are classically used: the so-called CRS (Constant Rate of Supply; Goldberg, 1963; Appleby and Oldfield, 1978;

Robbins *et al.*, 1978), CIC (Constant Initial Concentration; Pennington *et al.*, 1976) and CFCS (Constant Flux Constant Sedimentation rate; Goldberg, 1963; Krishnaswamy *et al.*, 1971) models. The choice of the appropriate model depends on ^{210}Pb profile shape (Appleby and Oldfield, 1983; Noller, 2000) but in some cases no dating is possible. The interbedding of rapid sedimentation deposits in slow sedimentation deposits is one of the possible causes of this impossibility. As this kind of deposit is of potential interest in palaeoclimatic (Chapron *et al.* 2002) and/or palaeoseismic (Smith and Walton, 1980; Doig, 1990; Doig, 1998; Chapron *et al.*, 1999; Noller, 2000) studies, solving the problem of dating sediment records with nonlinear ^{210}Pb vertical profiles is of wide interest.

In the 87-cm-long core ANT9902, taken in Lake Anterne (northern French Alps), the presence of many instantaneous deposits disturbs the ^{210}Pb profile, precluding the direct use of ^{210}Pb dating methods. The present contribution outlines an original approach, associating sedimentology and radiochemistry, in order to date this sedimentary record. First, a high-resolution sedimentological study applied to single-event deposits develops an understanding of their mechanism of formation. On the basis of the

mechanism determined, computed ^{210}Pb ages may then be correlated with historical events that could have triggered the instantaneous deposits. The ^{210}Pb profile and its estimates of the 'continuous' sedimentation rate may be further refined using the ages of the instantaneous deposits. This approach should thus provide chronostratigraphic marks indispensable to validate any ^{210}Pb geochronology (Smith, 2001).

Setting and analytical methods

Lake Anterne (2061 m) – located in the Sixt-Passy natural reserve, in the northern French Alps (Fig. 1) – is 600 m long, 400 m wide and its maximum depth is about 13 m. It is an oligotroph dimictic lake, ice-covered each winter from November to June. Tributaries essentially run over low-grade metamorphic Jurassic marls and shale. Gilbert-type deltas develop on major tributaries leading to the presence of steep foreset slopes. The 87-cm-long core ANT9902, which is discussed here, is one of the four sediment cores taken in Lake Anterne during the 1999 CALAMAR II coring survey (Desmet and Lignier, 1999). It was taken in the deepest part of the basin at 13.2 m water depth.

The lake's ^{210}Pb activity profile was obtained by measuring the

*Correspondence: F. Arnaud, Bilan et Processus en Domaine Sédimentaire UMR CNRS, Université de Lille 1, F-59655 Villeneuve d'Ascq Cedex, France. E-mail: fabien.arnaud@ed.univ-lille1.fr

†Present address: Renard Centre of Marine Geology, geological institute, Gent University, Gent, Belgium.

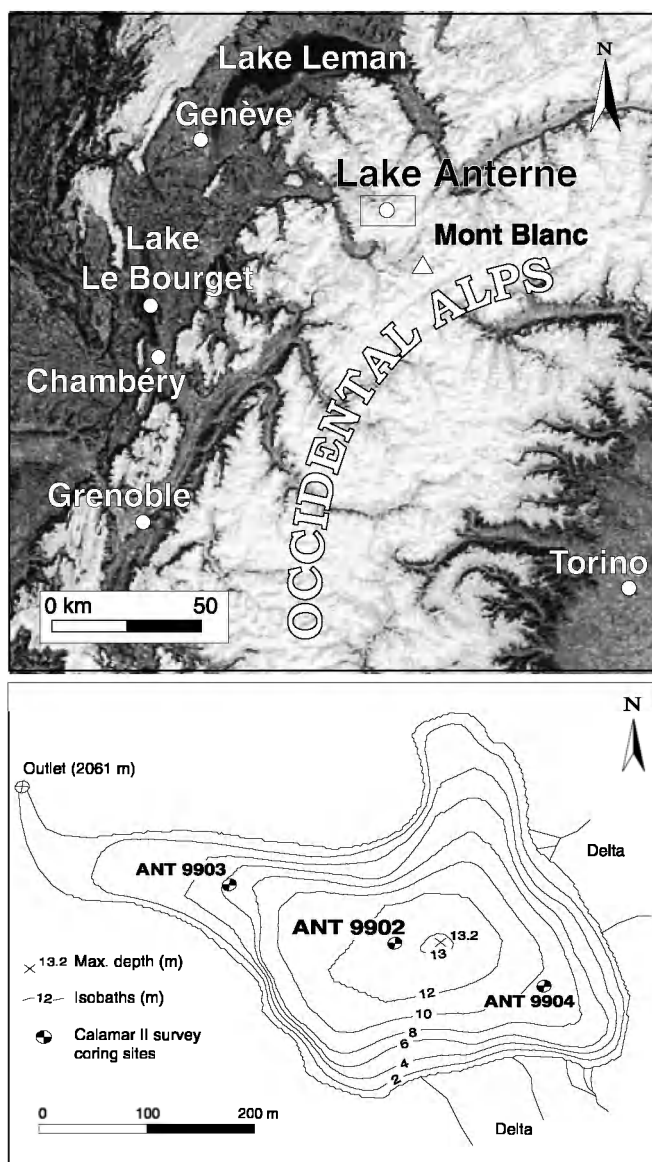


Fig. 1 The location of Lake Anterne in Occidental Alps and the three cores taken during the 1999 CALAMAR II survey. Core ANT9902, discussed in this paper, has been taken in the centre part of the basin, at 13.2 m water depth.

^{210}Po α -activity (Häsänen, 1977; detailed method and confidence assessment in Pourchet *et al.*, 1994) with a 5-mm sampling interval. ^{137}Cs activity was measured at each 1 cm depth increment by low-level gamma spectrometry (Pourchet and Pinglot, 1989). Micro-grain-size measurements were taken at 5-mm increments, all along the core, using a Malvern Micro-sizerTM. Grain-size parameters are a mean of 10 000 scans and measures

per sample. In order to characterize the depositional processes, the 'mean grain-size' $((Q_{10} + Q_{30} + Q_{50} + Q_{70} + Q_{90})/5)$ and 'sorting' $((Q_{75}/Q_{25})^{1/2})$ parameters were used. The CaCO_3 content was measured using a Bernard calcimeter. The clay content was determined using X-ray diffractograms obtained from orientated mounts from the carbonate-free clay fraction. The identified clay minerals were then semiquantitatively esti-

mated using MACDIFF[®] software (Petschick, 2001).

Results

Sedimentology

Core description and lithology. Core ANT9902 presents sharply laminated (~ 1 mm) fine-grained sediments interbedded with relatively thicker (1–4 cm) and coarser-grained layers (Fig. 2). Four lithofacies are recognizable in the core (Fig. 3A): facies 1 (f1) is characterized by the alternation of dark-grey and white millimetric laminae; facies 2 (f2) corresponds to 1- to 2-cm-thick white silty clay beds; facies 3 (f3) is made of pluricentimetric grey-coloured silty levels; and facies 4 (f4) is represented by 1- to 2-cm-thick dark-grey sandy beds sometimes containing vegetal debris.

The vertical organization of facies leads to distinguish the layers interbedded into laminated sediment (noted L) into two types of depositional sequences, as defined below (Fig. 3B):

- A-type sequences have a fining-upward, grain-supported, succession of facies f4, f3 and f2;
- B-type sequences comprise only facies f4 and f3, which are fining-upward too, but matrix-supported.

Microscopic observation of smear slides and measurement of CaCO_3 content reveal the preponderance of the siliciclastic fraction over biogenic compounds, both in laminae and interbedded layers. The clayey fraction is composed exclusively of illite and chlorite (Fig. 2) throughout the core. There is no observed relationship between clay mineral composition and the different facies.

Grain-size measurements. Facies f1 is relatively homogenous, characterized by clayey-silt deposits (mean size range: 11.6–24.5 μm) and sorting values ranging from 2 to 2.5 (Fig. 4). Facies f2 is the best sorted (sorting range: 1.8–2.3) and the finest grained (mean size range: 6–13.6 μm). For the f3 facies, grain-size data indicate the same mean size values both in A- and B-type sequences (mean size range – f3A: 13.6–31.2 μm ; f3B: 13.8–43.2 μm), samples from A-type sequences are

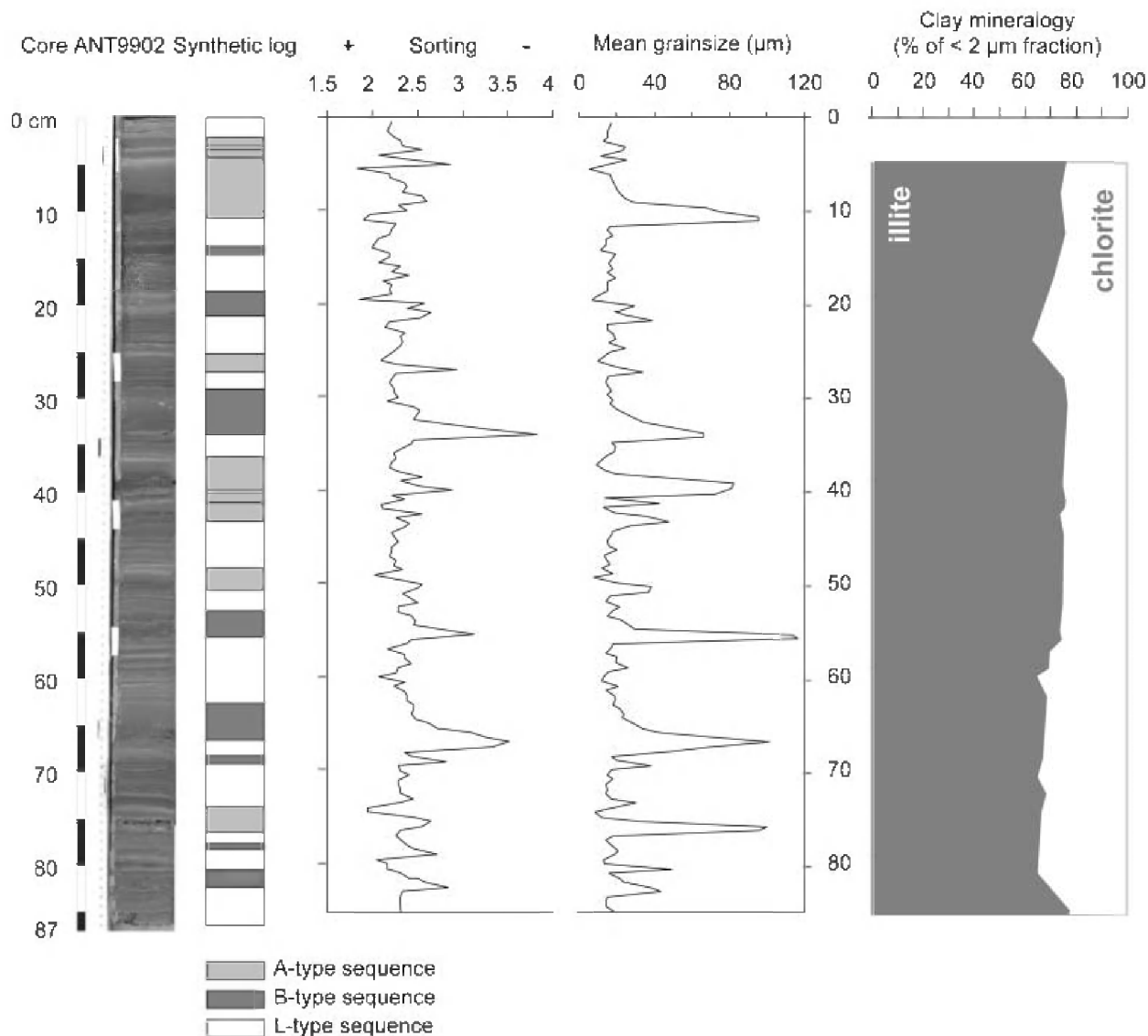


Fig. 2 Two different kinds of thick layers (A- and B-type sequences) are interbedded all along core ANT9902 in sharply laminated sediments. Grain-size parameters have been measured with a 5-mm sampling interval, sorting $((Q75/Q25)^{1/2})$ and mean grain-size $((Q10 + Q30 + Q50 + Q70 + Q90)/5)$ are presented here. Each peak of mean grain-size marks the bottom of an interbedded layer; they are associated with high sorting parameter values (poorly sorted sediment) only in B-type sequences.

slightly more sorted (sorting range: 2.1–2.6) than those from B-type sequences (sorting range: 2.2–2.9). Facies f4 from A- and B-type sequences also show similar mean grain-size values (mean size ranges – f4A: 23.3–99.9; f4B: 17.3–116.9), but sorting of samples from A-type sequences is marked (sorting ranges – f4A: 1.9–2.9; f4B: 2.4–3.8). Plotted in a mean size vs. sorting diagram (Fig. 4), A- and B-type sequences are clearly distinguishable at their base (f4) and similarly develop (f3). Samples from f2 levels, characteristic of A-type

sequences, are the finest grained and most sorted of the whole core.

Radiochemical measurements

The ^{210}Pb activity vs. depth curve is nonlinear (Fig. 5A) and thus cannot be interpreted to have resulted from radioactive decay alone. The activity of interbedded layers is particularly low compared with laminated layers and seems to be linked to grain-size variations: the fining-upward sequences are ^{210}Pb increasing. This pattern is particularly evident in the two A-type

sequences located between 3 and 10 cm-depth (Fig. 5A). Below 45 cm, the ^{210}Pb activity is roughly constant around a mean value of 0.022 bq kg^{-1} (Fig. 6) and represents the supported ^{210}Pb activity. ^{137}Cs γ -activity profile presents a sharp peak at 14.5 cm and is near to zero below 16 cm (Fig. 5B).

Interpretations

The Lake Anterne sedimentary system

Assuming that the sediments have the same source throughout the

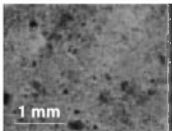
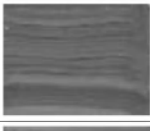
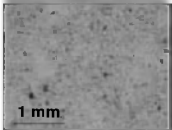

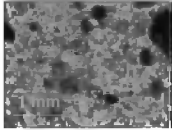
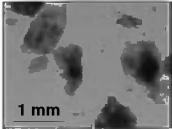

A			B					
Facies	Description	Smear slide observation	Sequence	Description	Image	Facies succession	Grain size	
							Mean size min. < mean < max. (µm)	Sorting min. < mean < max.
1	Sharply laminated light and dark clayey silt		L	Laminated deposits		1	11.6 < 16.8 < 24.5	2 < 2.3 < 2.5
2	White clay		A	Upward decreasing grain-supported sequence		2	6 < 11.4 < 13.6	1.8 < 2.1 < 2.7
3	brown to dark-grey clayey silt					3A	13.6 < 21.6 < 31.2	2.1 < 2.4 < 2.6
4	dark-grey silty sand					4A	23.3 < 58.2 < 99.9	1.9 < 2.5 < 2.9
			B	Upward decreasing matrix-supported sequence		3B	13.8 < 23.1 < 43.2	2.2 < 2.4 < 2.9
						4B	17.3 < 67.9 < 116.9	2.4 < 3.1 < 3.8

Fig. 3 Facies and sequences characteristics. (A) Facies definition is first based on macroscopic observations (colour, grain-size estimation). (B) The vertical organization of different facies and textural observations distinguish two different types of sequences (noted A and B) interbedded into laminated sediments (noted L): A-type sequences present the succession (from bottom to top) of facies 4, 3 and 2 and are grain-supported while B-type sequences present no top f2 facies and are matrix-supported. Grain-size analysis confirms this differentiation: B-type sequence basal deposits (f4B) present similar mean grain size (same facies) and are less sorted (different texture) than those from A-type sequences (f4A).

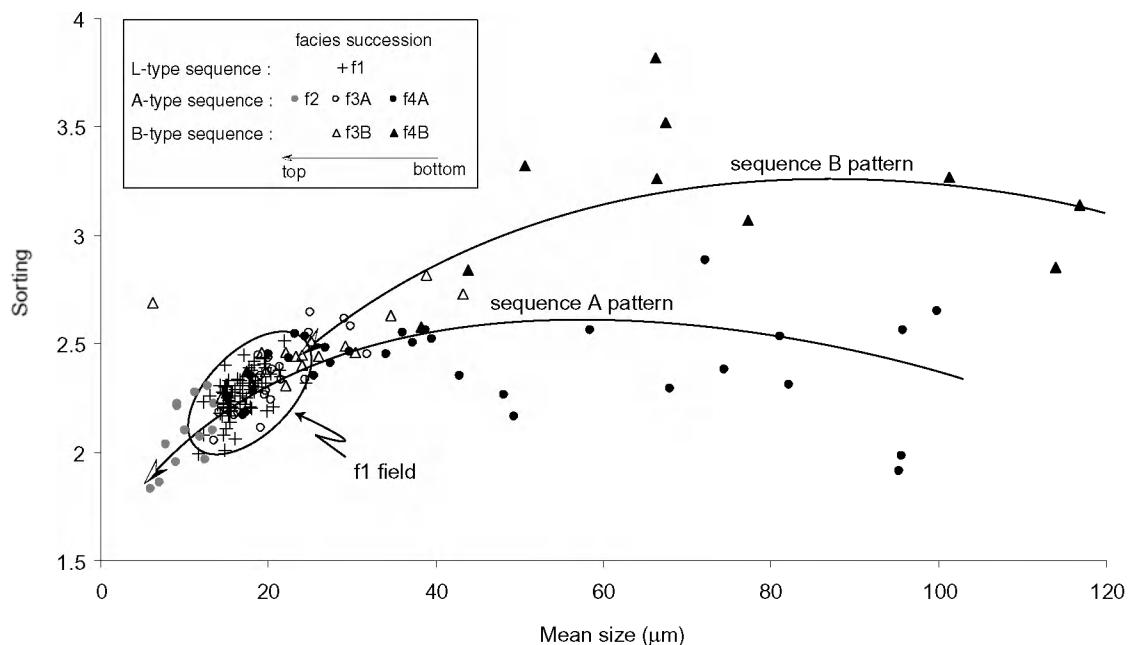


Fig. 4 Granulometric differentiation between sequences A and B. Plotting mean grain-size vs. sorting emphasizes the differences between A- and B-type sequences. Basal layers (f4) from sequence A are more sorted than those from sequences B, intermediate layers (f3A and f3B) and laminated sediments (f1) present the same signature and the top layers of sequences A (f2) are the more sorted and finest grained samples. Because of their relatively high sorting, f4A layers are interpreted as winnowed sediment deposited by a flood current; in contrast, facies f4B are matrix-supported sediments deposited by gravity reworking. The final term of sequences A (f2) represents the settling of the fine particles brought to the lake by the flood.

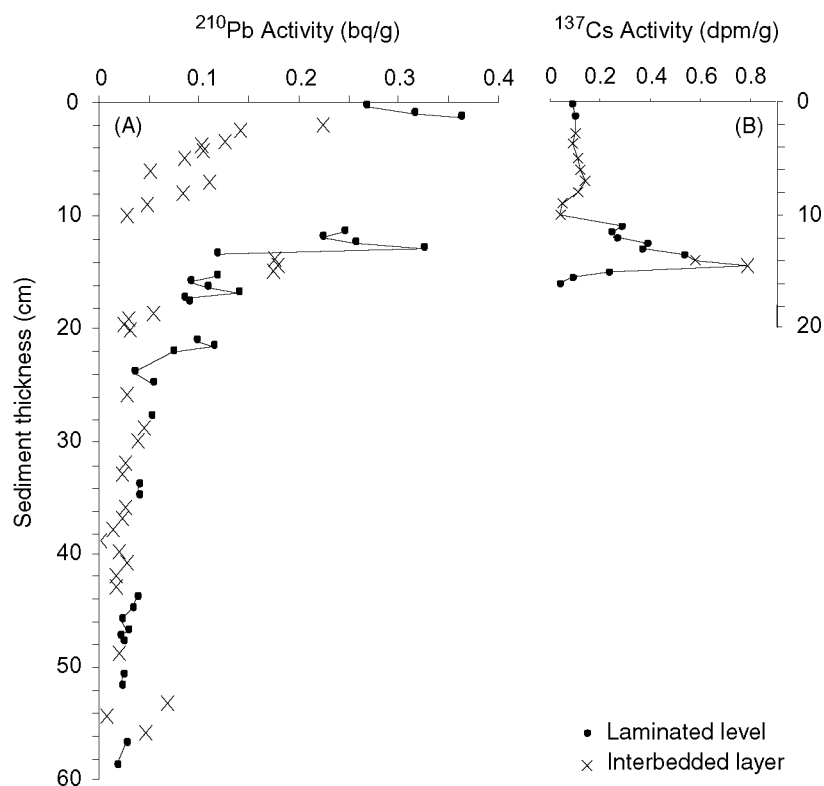


Fig. 5 ^{210}Pb (A) and ^{137}Cs (B) activity profiles. ^{210}Pb vertical profile is non-linear and thus cannot be interpreted as the result simply of radioactive decay. Depletions in ^{210}Pb values are correlated with the occurrence of A- and B-type sequences which can thus be interpreted as the cause of profile disturbance.

core – an assumption supported by constant clay mineralogy and CaCO_3 content – it is suggested that the differentiation between A- and B-type sequences must be driven by essentially different depositional processes. Compared to A-type, B-type sequences are characterized by the absence of a clayey f2 top-level, and by poorer sediment sorting (Fig. 4). The latter observation confirms the optical description of a matrix-supported sequence, suggesting that the transport energy is supplied by sediment weight rather than by a water current. Following the nomenclature of Mulder and Cochonat (1996), B-type sequences may thus be interpreted as fluidized or liquefied flow deposits of reworked sediment. Inversely, the good sorting of A-type sequences suggests that sediments have been winnowed by a water current, the fining-upward pattern having resulted from its decreasing velocity. Such a particle-loaded current may have resulted from an exceptional flood of the watershed

which would significantly increase the turbidity of the water column and lead to the deposition of a thick, fine-grained, well-sorted lamina (f2) during the following winter, when the lake is ice-covered.

Based on evidence described above, a revised sedimentological model is proposed for Lake Anterne. The three kinds of deposits defined above are linked to three different triggering mechanisms:

- Because of the regularity of their lamination, L-type sequences represent the continuous sedimentation of the lake;
- Winnowed sediments from A-type sequences are interpreted as major flood-event deposits;
- B-type matrix-supported sequences are sediment gravity-reworked and must be the consequence of natural collapse of steep slopes.

A- and B-type sequences are thus considered as single-event deposits interbedded within the continuous sharply laminated L-type sedimentation.

^{210}Pb data processing: age-depth relation

In order to understand and establish an age–depth relationship in the core, it is assumed first that laminated levels have been deposited by constant accumulation rate and that interbedded layers represent single-event deposits. Average accumulation rate (A.R.) is expressed as

$$\text{A.R.} = -\lambda/s, \quad (1)$$

where λ is the ^{210}Pb radioactive decay constant and s is the slope of the activity vs. depth curve.

A synthetic sedimentary record is then built composed only of the laminated levels, by removing the single event related layers from the original sedimentary record (Fig. 6). Plotted on logarithmic scale, the ^{210}Pb profile thus obtained can be considered as a straight line (determination coefficient is 0.92) with $s = 0.19 \text{ cm}^{-1}$. In such a case, the CFCS model (Goldberg, 1963; Krishnaswamy *et al.*, 1971) can be used and (1) provides an A.R. of $1.6 \pm 0.1 \text{ mm yr}^{-1}$ (see Fig. 6 caption for discussion of confidence limits).

It is assumed that each A-type sequence represents an annual sedimentation cycle (flood event plus winter settling of fine particles) and that B-type deposits occur instantaneously. Accordingly, the extrapolation of calculated A.R. to all of the laminated levels in the original record permits the construction of an age–depth relationship (Fig. 7).

Discussion: chronological control

1963 Nuclear weapon tests maximum

The CFCS model provides the date AD 1963 ($\pm 2 \text{ yr}$) to the ^{137}Cs peak located at 14.5 cm depth (Fig. 5B). It can thus be attributed to the AD 1963 maximum ^{137}Cs emission from atmospheric nuclear weapons tests. The decreasing ^{137}Cs pattern above 14.5 cm is characteristic of the end of the 60 s when the number of atmospheric nuclear tests decreases. The sharpness of this peak, together with the lamination of sediment, indicates that no bioturbation affects the sediment record.

In the monotonous ^{137}Cs profile from 0 to 10 cm-depth the Chernobyl accident (AD 1986) does not stand out

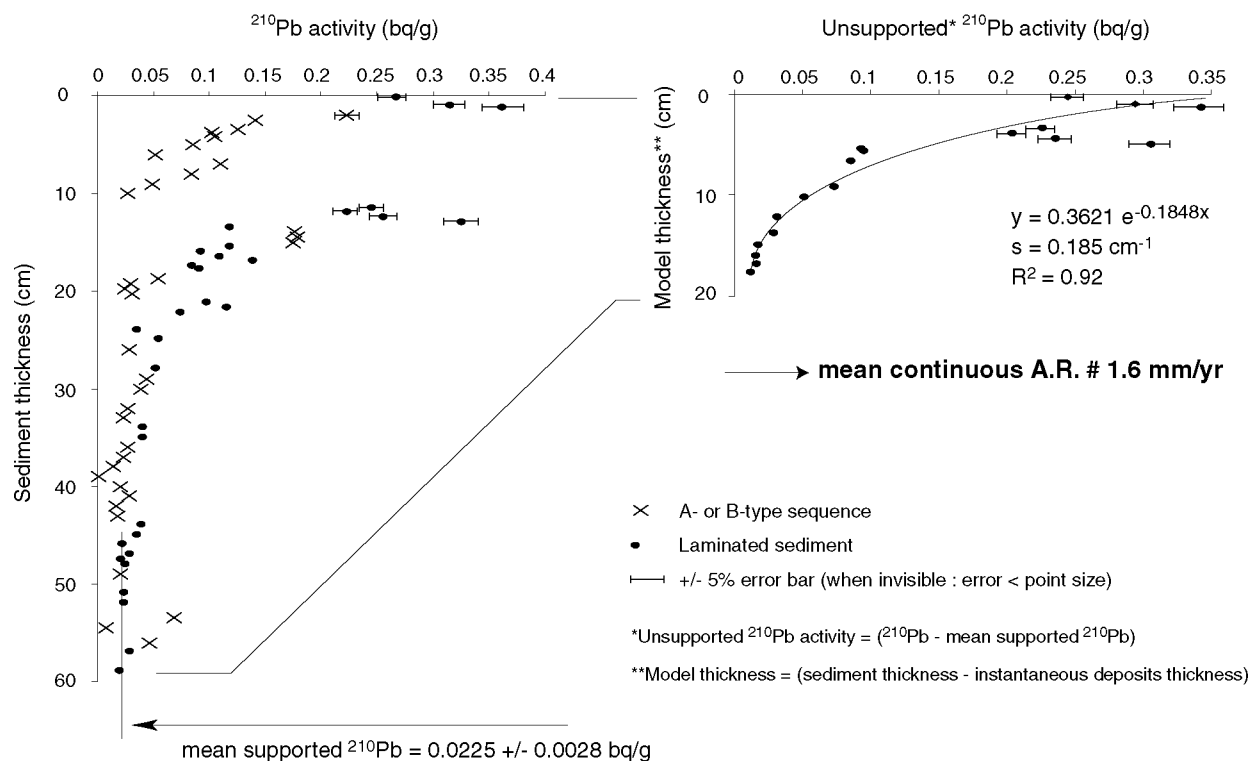


Fig. 6 ^{210}Pb data processing. As A- and B-type sequences have been interpreted as single-event deposits, they do not record time in the same way that laminated sediments do. Removing these events from the unsupported ^{210}Pb profile makes it linear in a semilog graph, following the radioactive decay law with an acceptable determination coefficient of 92%. Because the synthetic unsupported ^{210}Pb profile presents a logarithmic relation with depth, the CFCS model is applied (Appleby *et al.*, 1983; Noller, 2000) and provides an accumulation rate of about 1.6 mm yr^{-1} which represents the average accumulation rate of continuous sedimentation as opposed to single-event linked sedimentation. The uncertainty of ^{210}Pb α -activity measurement is less than 5% (Pourchet *et al.*, 1994) and is negligible compared to model assumptions. Supported ^{210}Pb activity is the mean of a series of eight values with similar grain-size (values from the deepest instantaneous deposit have been rejected) and low standard deviation (0.003). The confidence interval (95%) is $0.0225 \pm 0.0028 \text{ Bq g}^{-1}$. Taking account of this uncertainty, the accumulation rate is $1.58 \pm 0.1 \text{ mm yr}^{-1}$. Owing to sampling interval and model assumptions, a $< 0.1 \text{ mm yr}^{-1}$ precision is unrepresentative; in the age–depth relationship the value $1.6 \pm 0.1 \text{ mm yr}^{-1}$ is used as a reasonable approximation of this computed value.

(Fig. 5B). The predicted depth of year 1986 is around 3 cm, just between two thin flood-event deposits. If the flood deposit located between 2 and 2.6 cm-depth occurred during the AD 1986 spring, the related surface current might have brought ^{137}Cs -loaded fine particles out of the lake, thus hiding the Chernobyl ^{137}Cs signature.

Historical seismic activity

B-type sequences are related to collapses of steep slopes that are most likely to be related to local seismic activity (Doig, 1990; Ouellet, 1997; Doig, 1998).

Lignier (2001) showed the locally greatest earthquake intensity felt during the last three centuries (database from Lambert and Levret-Albaret, 1996) around Lake Anterne should

have been caused by the seismic events of AD 1905 (Emosson, Switzerland), 1855 (Visp, Switzerland), 1817 (Chamonix, France) and 1755 (Brigg, Switzerland). These ages show good agreement with the computed ages of the four thickest B-type sequences (Fig. 7), thus allowing the conclusion that they were triggered by the locally significant earthquakes of the past two centuries.

With each seismically induced B-type sequence as a chronostratigraphic mark, revised accumulation rates are calculated for intervals between each of them (Fig. 7). Accumulation rate variations thus computed are consistent with variations of lithogenic flux recorded in Lake Cornu (Desmet *et al.*, 2001), 5 km far from Lake Anterne. Those variations seem to be in response to climate

change following the Little Ice Age (AD 1350–1850). In both Lake Anterne and Lake Cornu the period before AD 1855 yields low accumulation rates (Lake Anterne A.R. 1.2 mm yr^{-1}) suggesting low erosion rates following snow accumulation in the lake watershed during the summer. By contrast, AD 1855–1905 is a period of intense melting, leading to an increasing lithogenic sediment flux (Lake Anterne A.R. 1.8 mm yr^{-1}). The twentieth century, since 1905 AD, is a period of intermediate erosion rate (Lake Anterne A.R. 1.6 mm yr^{-1}).

Conclusions

The data processing protocol described in this paper allows for the development of an age–depth curve based on ^{210}Pb estimation of continuous

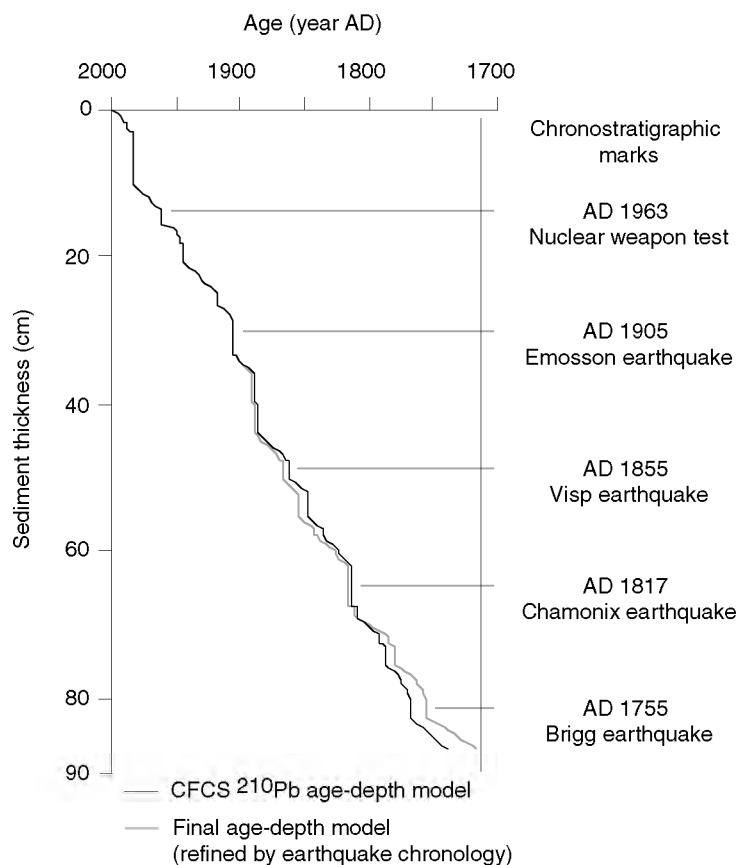


Fig. 7 Age–depth relationship. A first age–depth model (black line) can be established considering laminated sediments have been deposited by a constant accumulation rate. This A.R. (1.6 mm yr^{-1}) is given by the ^{210}Pb CFCS Model (Fig. 5). In this model, vertical lines correspond to instantaneous deposits: flood deposits and gravity reworking, representing, respectively, a time increment of 1 and 0 years (explanations in text). This model is constrained over the 20th century by the identification of the AD 1963 ^{137}Cs peak associated with atmospheric nuclear weapon tests and by the correlation between a thick gravity reworking deposit and the AD 1905 Emosson earthquake. Deeper in the sediment, the correlation of the three thicker B-type sequences with the three major earthquakes historically recorded in the surrounding area allows us to propose a refined age–depth model (grey line) by considering the earthquake-induced deposits as chronostratigraphic markers. This refining brings out accumulation rate variations which are consistent with lithogenic input variations recorded in Lake Cornu (Desmet *et al.*, 2001) and interpreted as a response to the end of the Little Ice Age (explanations in text).

sedimentation rate instead of average bulk accumulation rate, where classical ^{210}Pb dating models would have been inefficient. This paper demonstrates an approach to understanding age/accumulation relationships in sedimentary systems by applying ^{210}Pb chronology to dating sediment records that exhibit abrupt changes in accumulation rate.

Correlation of historical events, in this case earthquakes, to sedimentary ^{210}Pb profiles leads to the identification of fluctuations in accumulation

rate which are likely related to climate variability. This demonstrates that average accumulation rate must be used carefully when establishing age models of high-resolution proxy time-series. In order to be accurate and of wide use, studies of climate short-term variability, often highlighting several-year-long cycles, require multiple lines of evidence to constrain age models by taking into account instantaneous deposits and accumulation rate variability.

Radiometric and sedimentological evidence validate the proposed age model in the particular case of Lake Anterne, although there is no evidence it would work in other similar sediment records. The process explained here needs to be tested further in other lakes.

Acknowledgements

We wish to thank Jay S. Noller for his constructive review. Grateful thanks to Olivier Radakovitch who brought critical and constructive observations to this paper. This work was partly founded by an ACP grant from CNRS. Authors are grateful to the ASTER, particularly to Mrs J. Vodihn and to the guards from Sixt-Passy and Aiguilles Rouges reserves, which provided financial and technical support to CALAMAR coring surveys since 1998.

References

- Appleby, P.G. and Oldfield, F., 1978. The calculation of ^{210}Pb dates assuming a constant rate of supply of unsupported ^{210}Pb to the sediment. *Catena*, **5**, 1–8.
- Appleby, P.G. and Oldfield, F., 1983. The assessment of ^{210}Pb data from sites with varying sediment accumulation rates. *Hydrobiology*, **103**, 29–35.
- Chapron, E., Beck, C., Pourchet, M. and Decoininck, J.F., 1999. 1822 earthquake-triggered homogenite in Lake Le Bourget (NW Alps). *Terra Nova*, **11**, 86–92.
- Chapron, E., Desmet, M., De Putter, T. *et al.*, 2002. Climate variability in the NW Alps, France as evidenced by 600 years of terrigenous sedimentation in Lake Le Bourget. *Holocene*, **12–2**, 177–185.
- Desmet, M. and Lignier, V., 1999. *Mission CALAMAR II Rapport de Mission*. LGCA, Chambéry.
- Desmet, M., Devie, C., Pourchet, M. *et al.*, 2001. High Mountain Lakes Sediment Records: Evidence for Multi-Decennial Oscillations of Climate and Anthropogenic Impact during the Last Millennium. In: *Proceedings of EUG XI Strasbourg*, 6(1), p. 128.
- Doig, R., 1990. 2300 yrs history of seismicity from silting events in Lake Tadoussac, Charlevoix, Québec. *Geology*, **18**, 820–823.
- Doig, R., 1998. 3000-years paleoseismological record from the region of the 1998 Saguenay, Québec, Earthquake. *Bull. Seism. Soc. Am.*, **88**, 1198–1203.
- Goldberg, E.D., 1963. Geochronology with lead-210. In: *Radioactive Dating*, pp. 121–131. IAEA, Vienna.

- Häsänen, E., 1977. Dating of sediments, based on ^{210}Po measurements. *Radiochem. Radioanalyt. Letts*, **31**(4–5), 207–214.
- Krishnaswamy, S., Lal, D., Martin, J.M. and Meybeck, M., 1971. Geochronology of lake sediments. *Earth Planet. Sci. Lett.*, **11**, 407–414.
- Lambert, J. and Levret-Albaret, A., 1996. *Mille ans de séismes en France*. Ouest éditions, Nantes.
- Lignier, V., 2001. *Mécanismes et conditions de l'enregistrement de la sismicité dans les sédiments lacustres*. Unpubl. doctoral dissertation, Université de Savoie.
- Mulder, T. and Cochonat, P., 1996. Classification of offshore mass movements. *J. Sedim. Res.*, **66**(1), 43–57.
- Noller, J.S., 2000. Lead-210 Geochronology. In: *Quaternary Geochronology Methods and Applications* (J. S. Noller et al., eds), AGU Reference Shelf 4, pp. 115–120. American Geophysical Union, Washington.
- Ouellet, M., 1997. Lake sediments and Holocene seismic hazard assessment within the St Lawrence Valley, Québec. *Bull. Geol. Soc. Am.*, **109**, 631–642.
- Pennington, W., Cambray, R.S., Eakins, J.D. and Harkness, D.D., 1976. Radiocnuclide dating of the recent sediments from Blelham Tarn. *Freshw. Biol.*, **6**, 317–331.
- Petschick, 2001. *MacDiff*® software notice. At <http://www.geol.uni-erlangen.de/html/software/soft.html>.
- Pourchet, M. and Pinglot, J.F., 1989. Cesium 137 and lead 210 in Alpine lake sediments: measurements and modelling of mixing processes. *J. Geophys. Res.*, **94C**(9), 12,761–12,770.
- Pourchet, M., Mourguiart, P., Pinglot, J.F. et al., 1994. Sédimentation récente dans le lac Titicaca (Bolivie). *C. R. Acad. Sci. Paris*, **319**, 535–541.
- Robbins, J.A., Edgington, D.L. and Kemp, K.L.W., 1978. Comparative ^{210}Pb , ^{137}Cs and pollen geochronologies from lakes Ontario and Erie. *Quat. Res.*, **10**, 256–278.
- Smith, J.N., 2001. Why should we believe ^{210}Pb sediment geochronologies? *J. Environ. Rad.*, **55**, 121–123.
- Smith, J.N. and Walton, A., 1980. Sediment accumulation rates and geochronologies measured in the Saguenay Flord using the Pb-210 dating method. *Geochim. Cosmochim. Acta*, **44**, 225–240.
- Von Grafenstein, U., Erlenkeuzer, H., Müller, J., Trimborn, P. and Alefs, J., 1996. A 200 year mid-European air temperature record preserved in lake sediments: an extension of the $\delta^{18}\text{O}_p$ -air temperature relation into the past. *Geochim. Cosmochim. Acta*, **60/21**, 4025–4036.

Received 16 October 2001; revised version accepted 7 March 2002